

THREE-DIMENSIONAL MATHEMATICAL (DYNAMIC) MODEL OF THE SINTERING PROCESS. PART I

Yu. A. Frolov¹ and L. I. Polotskii²

UDC 669.162.16

A three-dimensional mathematical (dynamic) model is presented to describe the sintering process. The model was developed to solve theoretical and practical problems. It allows real-time determination of the dynamic distribution of the temperature and chemical composition of the charge, the melt, the sinter cake, and the gas in the bed with allowance for transients, as well as the temperatures in the pallets and the parameters of the gas flow in the flue channel – including air infiltration.

Keywords: *three-dimensional (dynamic) mathematical model, sintering process, sintering machine, gas, moisture content, reduction, gas dynamics, evaporation, condensation, heating, oxidation, cooling, melting, filtration rate, temperature, fuel, chemical composition, charge.*

For the foreseeable future, the sintering of iron ores and concentrates will remain the main method that is used to prepare metallurgical raw materials for smelting in blast furnaces. Over the course of sintering's existence, a substantial amount of experimental data has been accumulated on this process both in the laboratory and in factory tests. At the same time, modern tools – mathematical models – need to be used to analyze the process theoretically, solve problems encountered in the design of new sinter plants and the reconstruction of existing plants, and optimize the sintering operation.

A substantial number of experimental-theoretical and theoretical studies have been devoted to studying heat- and mass-transfer processes that take place in the bed of charge materials on sintering machines. Wendeborn [1] was the first to note that heat and mass transfer during sintering cannot be analyzed based on the total heat balance of the process. Instead, Wendeborn used the heat balance in the fuel-combustion zone and showed that heat is transferred over the height of the bed by gas convection and by conduction. Fuel combustion and heat transfer during sintering were analyzed by Voice and Wild [2] with the use of two indices: the rate of propagation of the combustion front (the moment at which there is an abrupt rise in temperature after ignition of the fuel) and the rate of propagation of the “heat-transfer front” (the rate of propagation of the maximum temperature over the height of the bed). To do this, the researchers conducted several series of original and illustrative experiments and established the role of each of these indices.

In addition to the investigations already mentioned, a large number of theoretical studies have been devoted to mathematically describing local processes that take place during the sintering of the charge. The studies are based on material and heat balances constructed with allowance for certain empirical relations between the input and output parameters. These relations are substitutes for the kinetic laws that govern the processes. They do not reveal anything new about the physics of the sintering operation and are valid only within narrow ranges of the parameters' values, which is the main shortcoming of balance methods.

¹ Uralklektra Scientific and Production Enterprise, Ekaterinburg, Russia; e-mail: uaf.39@mail.ru.

² Ural Institute of Metals, Ekaterinburg, Russia; e-mail: mlpol@mail.ru.

The principles expounded by Anzelius [3] and Schuman [4] for the mathematical modeling of heat transfer in a bed of charge materials injected with a gaseous medium made it possible to calculate the temperatures that exist during the heating of thermally thin particles in the bed. The solutions that were obtained have been used to construct diagrams for calculating the temperatures of the gas and the charge materials. Although this method is somewhat coarse, it makes it possible to obtain a first approximation of the temperature field in processes that take place in layered materials.

The study performed by Bratchikov et al. [5] involved the use of a scheme for layer-by-layer fuel combustion that accounts for specific features of the sintering process (the decomposition of carbonates, the occurrence of oxidation-reduction reactions, etc.). The fuel-combustion zone is calculated based on heat-balance equations, while heat transfer in the upper and lower regions of the bed are calculated in accordance with a fixed-bed scheme based on the methods in [3, 4]. The refined method described in [5, 6] uses the heat balance in the combustion zone but calculates heat transfer in accordance with a countercurrent scheme, while an expanded heat-engineering analysis of the sintering process was performed in [7, 8]. However, the model that was used did not account for the kinetics of the reactions over the height of the fuel-combustion zone.

In [7], Shklyar et al. presented a mathematical model of heat and mass transfer and gas dynamics in the bed of charge materials on a sintering machine. It was the most complete such description that had been given up to that point, considering the state of computer technology at the time. The model accounted for the kinetics of fuel combustion over the height of the bed, heat transfer by conduction over the bed's height, the kinetics of the drying and re-moistening of the bed, thermal effects and the kinetic laws governing the decomposition of limestone, the melting of the charge, the crystallization of the melt, the occurrence of oxidation-reduction reactions, the gas dynamics of the bed, and heat transfer in the pallets. At the same time, the model was static and made no allowance for changes in the distributions of the coarseness and bulk density of the charge and the fuel over the height of the bed.

Later, several researchers – specifically, Cumming and Thurlby [8], Nath, Silva, and Chakraborti [9], and Mitterlehner et al. [10] – also constructed static mathematical models of the sintering process in a 2D format.

The next advance was the construction of three-dimensional mathematical models of the thermal and gas-dynamic performance of sintering machines [11–13]. The three-dimensional model created by Castro et al. [13] accounted for gas dynamics, convective and radiative heat transfer, the kinetics of the evaporation and condensation of moisture, the combustion of the fuel and the decomposition of carbonates, oxidation-reduction reactions, shrinkage of the bed, melting of the charge and crystallization of the melt, and phase transformations. However, this was also a static model, and it was refined on the basis of laboratory test results rather than factory test data. In addition, the model did not account for the nonuniformity of the sintering process across the width of the bed, heat transfer in the pallets, the infiltration of air into the gas flue, the parameters of the gas in the flue in the presence of gas-cleaning equipment, or the characteristics of the exhausters. The model has been used to evaluate emissions of hazardous substances into the atmosphere.

The three-dimensional mathematical (dynamic) model that we developed to describe the sintering of a charge and cooling of the sinter on sintering machines is a program that makes it possible to determine the dynamic distribution of the charge's temperature and chemical composition, the quantity of molten material that is present, and the temperature, chemical composition, and gasdynamic parameters of the gas within the volume of the bed. The program also determines the temperature distribution in the pallets and the parameters of the gas with air infiltrating the vacuum chambers and the flue of a sintering machine equipped with exhausters.

We chose to use a *frontal model* to describe the chemical reactions in the bed.

Algorithm of the Model. The notation: h – height of the bed; L – distance from the charging section of the sintering machine; t – temperature; w – velocity of the front in a lump of charge material; v – velocity of the gas; Q – heat content, heat source; K – concentration of particles; ρ – density; c – specific heat; λ – thermal conductivity; γ – the drag coefficient of the bed; d_c – the fraction of the charge in the heat flow from combustion of the coke; d_{CO_2} – the fraction of CO_2 in the coke-combustion products; the subscripts Ca, Mg, Fe, c, ch, gf, he, com, r, evp, mel, st, and loss, respectively, refer to $CaCO_3/CaO$, $MgCO_3/MgO$, Fe_2O_3/FeO , coke, the charge, the gas flow, heat exchange, combustion, reactions, evaporation, melting, steam, and losses.

The granules of the material comprising the ore-bearing part of the charge are regarded as spheres of a prescribed diameter, and the $CaCO_3/CaO$, $MgCO_3/MgO$, and Fe_2O_3/FeO fronts move inside these spheres. A particle of the solid fuel is assumed

to be a sphere of a variable diameter that decreases as the combustion of the carbon proceeds. The velocities of the reaction fronts in the particles are functions of the temperature of the material. The chemical composition of the gas and the heat sources and sinks are calculated in accordance with the changes that occur in the chemical composition of the charge as the above-mentioned fronts move. The rate of heat transfer between the gas and the charge depends on the velocity of the gas and is directly proportional to the total surface area of the particles comprising the ore-bearing part of the charge and the solid fuel.

The sintering process is described by a system of partial differential equations for the parameters of the charge and by ordinary differential equations for the parameters of the gas flow:

the diameter of a granule of CaCO_3 :

$$\frac{\partial D_{\text{Ca}}}{\partial \tau} + \frac{\partial D_{\text{Ca}}}{\partial L} v_{\text{ch}} = w_{\text{Ca}}(t_{\text{ch}}); \quad (1)$$

the diameter of a granule of MgCO_3 :

$$\frac{\partial D_{\text{Mg}}}{\partial \tau} + \frac{\partial D_{\text{Mg}}}{\partial L} v_{\text{ch}} = w_{\text{Mg}}(t_{\text{ch}}); \quad (2)$$

the diameter of the FeO front:

$$\frac{\partial D_{\text{Fe}_1}}{\partial \tau} + \frac{\partial D_{\text{Fe}_1}}{\partial L} v_{\text{ch}} = w_{\text{Fe}_1}(t_{\text{ch}}); \quad (3)$$

the diameter of the Fe_2O_3 front:

$$\frac{\partial D_{\text{Fe}_2}}{\partial \tau} + \frac{\partial D_{\text{Fe}_2}}{\partial L} v_{\text{ch}} = w_{\text{Fe}_2}(t_{\text{ch}}); \quad (4)$$

the diameter of the unburned part of the coke:

$$\frac{\partial D_{\text{c}}}{\partial \tau} + \frac{\partial D_{\text{c}}}{\partial L} v_{\text{ch}} = w_{\text{c}}(t_{\text{ch}}); \quad (5)$$

the heat content of the charge:

$$\begin{aligned} \frac{\partial Q_{\text{ch}}}{\partial \tau} + \frac{\partial Q_{\text{ch}}}{\partial L} v_{\text{ch}} = & -Q_{\text{he}} + Q_{\text{com}} d_{\text{ch}} + Q_{\text{rFe}} - \\ & - Q_{\text{rCa}} - Q_{\text{rMg}} - Q_{\text{evp}} - Q_{\text{mel}} + \lambda \frac{\partial^2 t_{\text{ch}}}{\partial h^2}; \end{aligned} \quad (6)$$

the moisture content of the charge:

$$\frac{\partial W_{\text{ch}}}{\partial \tau} + \frac{\partial W_{\text{ch}}}{\partial L} v_{\text{ch}} = Q_{\text{evp}} / 595; \quad (7)$$

the volumetric flow rate of carbon dioxide:

$$\begin{aligned} \frac{dV_{\text{CO}_2}}{dh} = & K_{\text{ch}} \pi D_{\text{Ca}}^2 \frac{dD_{\text{Ca}}}{d\tau} \rho_{\text{Ca}} / 100 \cdot 22.4 + K_{\text{ch}} \pi D_{\text{Mg}}^2 \frac{dD_{\text{Mg}}}{d\tau} \rho_{\text{Mg}} / 84 \cdot 22.4 + \\ & + K_{\text{c}} \pi D_{\text{c}}^2 \frac{dD_{\text{c}}}{d\tau} \rho_{\text{c}} / 12 \cdot 22.4 d_{\text{CO}_2} + K_{\text{ch}} \pi D_{\text{Fe}_2}^2 \frac{dD_{\text{Fe}_2}}{d\tau} \rho_{\text{Fe}_2} / 160 \cdot 22.4; \end{aligned} \quad (8)$$

the volumetric flow rate of CO:

$$\frac{dV_{\text{CO}}}{dh} = K_c \pi D_c^2 \frac{dD_c}{d\tau} \rho_c / 12 \cdot 22.4(1 - d_{\text{CO}_2}) - K_{\text{ch}} \pi D_{\text{Fe}_2}^2 \frac{dD_{\text{Fe}_2}}{d\tau} \rho_{\text{Fe}_2} / 160 \cdot 22.4; \quad (9)$$

the volumetric flow rate of steam:

$$\frac{dV_{\text{H}_2\text{O}}}{dh} = \frac{dW_{\text{ch}}}{d\tau} / 18 \cdot 22.4; \quad (10)$$

the volumetric flow rate of oxygen:

$$\frac{dV_{\text{O}_2}}{dh} = K_{\text{ch}} \pi D_{\text{Fe}_1}^2 \frac{dD_{\text{Fe}_1}}{d\tau} \rho_{\text{Fe}_1} / 288 \cdot 22.4 + K_c \pi D_c^2 \frac{dD_c}{d\tau} \rho_c / 12 \cdot 22.4(0.5 + d_{\text{CO}_2} / 2); \quad (11)$$

the vacuum:

$$\frac{dP}{dh} = \gamma \rho_{\text{gf}} v_{\text{gf}}^2; \quad (12)$$

the heat content of the gas:

$$\frac{dQ_{\text{gf}}}{dh} = Q_{\text{he}} + Q_{\text{com}}(1 - d_{\text{ch}}) + Q_{\text{st}} - Q_{\text{loss}}. \quad (13)$$

The temperature of the charge (and the temperature of the gas) are calculated based on the values found for heat content:

$$t_{\text{ch}} = Q_{\text{ch}} / (\rho_{\text{ch}} c_{\text{ch}}); \quad (14)$$

$$t_{\text{gf}} = Q_{\text{gf}} / (\rho_{\text{gf}} c_{\text{gf}}). \quad (15)$$

The drag coefficient of the bed is assigned a value in the file of initial data. During calculations, it is used together with corrections for the state of the bed (moist/dry/caked) and the position of a calculated point across the width of the bed. The dependence of the drag coefficient on porosity is taken into account, since porosity is a function of the coordinate in the bed's width direction.

Thermal conductivity inside the bed is assumed to be zero, due to the low rate of contact heat transfer in the charge compared to the rate of convective heat transfer. The coefficients of heat transfer from the bed to the grates of the pallets and from the grates and the gas to the beams under the grates were determined in the course of the model's adaptation.

The equations of heat and mass transfer are solved on a three-dimensional difference grid in the region occupied by the bed of charge materials. The sintering process can be calculated either in the packet regime or in the interactive regime. The following are assigned values in the file of initial data: the geometric characteristics of the sintering machine; the rate-related parameters (the speed of the sintering-machine strand, the composition and rate of consumption of the charge materials, the distribution of the input characteristics of the charge over the height of the bed, and the rate of flow of natural gas in the hearth); the parameters and characteristics of the chemical reactions and heat transfer; computational parameters (the mesh of the grid, the time step, and the accuracy parameters of the iteration processes).

The results of the calculations are visualized by having the display show a colored chart that illustrates the calculated fields of the process parameters for longitudinal and transverse sections of the bed. The position of the sections along the sintering machine can change during the computation. Figure 1 presents an example of visualization for a sintering machine at the Celyabinsk Metallurgical Combine (ChMK) that has a total area of 240 m² and a sinter-cooling zone (138/102 m²). The temperatures of the material and the gas, the quantity of molten material, and the percentage contents of FeO, Fe₂O₃, C, O₂, CO, and CO₂ can also be brought up on the display. During the computation, it is possible to change the height of the

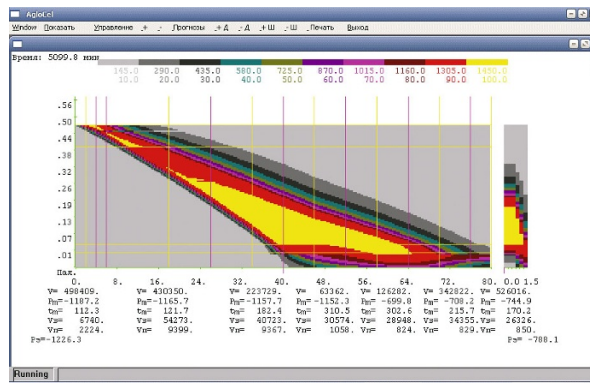


Fig. 1. Visualization of the analysis of the sintering process on a sintering machine with zone cooling (length of the sintering zone 46 m, length of the cooling zone 34 m): V – gas flow rate in the collecting mains of the zones, nm^3/h ; p_m – vacuum in the mains, dPa ; t_m – temperature of the outgoing gases, $^{\circ}\text{C}$.

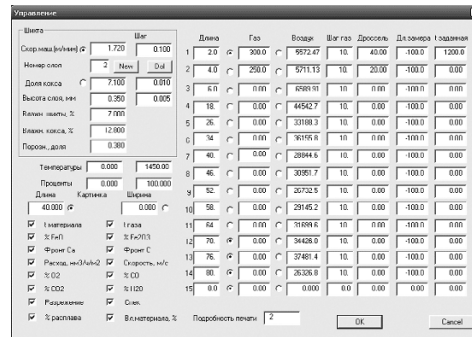


Fig. 2. Control panel for the model.

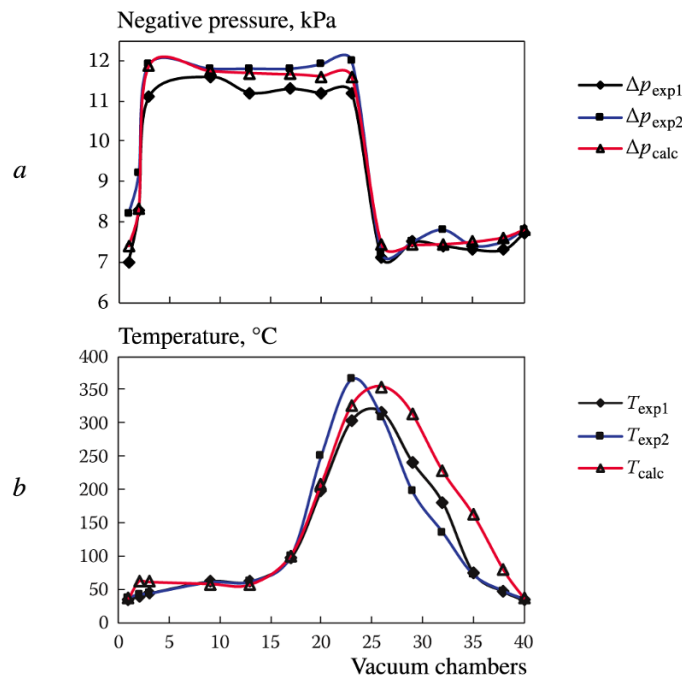


Fig. 3. Results from adaptation of the model based on the negative pressure (a) and temperature (b) of the gases in the vacuum chambers during operation of the sintering machine in two characteristic regimes.

TABLE 1. Theoretical-Experimental Operating Parameters of a Sintering Machine in the Base Regime

Parameter	Charge-sintering zone	Cake-cooling zone	Total
Area, m ² /%	138/57.5	102/42.5	240/100
Number of vacuum chambers	23	17	40
Width of the pallets, m		3.0	
Height of charge bed, mm		460	
including the bottom layer, mm		30	
Pallet speed, m/min		1.72	
Sintering-machine productivity, tons/h		149.65	
Unit sintering-machine productivity, tons/(m ² ·h)		1.084	
Productivity of the blowers, m ³ /min	13100	15250	
Gas temperature ahead of the blowers, °C	119	166	
Increase in blower pressure, kPa	12.32	8.22	
Temperature of the cake at the end of the sintering operation, °C:			
average over the cross section of the layer	598		
average over the height at the center of the layer	684		
Temperature of the cake when it leaves the strand, °C:			
average		18	
at the center		23	
maximum (bottom of the bed)		56	
Location where fuel combustion ends, m		39.0	
Power consumed by the blowers, kW	3496	3086	6582
Unit electric-power consumption, kWh/ton	23.36	20.62	43.98
FeO in the sinter, wt.%		12.20	12.2
Unit fuel consumption, kg/ton (dry)	56.58		56.58

bed, the speed of the strand, the natural-gas and air flow rates, and the parameters that characterize the choking of the vacuum chambers (these parameters are shown in Fig. 2 for the same sintering machine just mentioned). Numerical values for the calculated fields of the following parameters can be sent to a text file at any moment during the computation: the temperatures of the material and the gas, the contents of FeO and Fe₂O₃, the position of the CaCO₃ front and the C front, gas flow rate, gas filtration rate, the vacuum in the bed and in the flue with allowance for air infiltration, the contents of O₂, CO, CO₂, and H₂O in the gas inside the bed and the flue, and the amounts of molten material and caked material that have been formed. The total and running material and heat balances for the sintering operation are sent to the file at the same time. The parameters of the sintering process along the sintering machine are entered into another text file.

The program written for the model offers more flexibility than the model described in [14]:

- 1) the sintering machine can be divided into two zones – the zone in which the charge is sintered and the zone in which the sinter cake is cooled; each of these zones has its own flue channel;
- 2) the lengths of the sintering and cooling zones can be changed based on the number of vacuum chambers in each zone and the dimensions of the flue channel;

TABLE 2. Total Material Balance

Elements in the charge and the gas	Input		Output		
	kg/h	nm ³ /h	kg/h	nm ³ /h	%
Inert elements	94061.2		94061.2		
CaCO ₃	16	834.1	55.2		
FeO	38	806.1	31869.8		
CaO	13	819.2	23215.5		
MgO	3162.9		3162.9		
Fe ₂ O ₃	138679.8		146386.4		
Coke fines	8466.9		1526.3		
Water	16880.0		0.0		
N ₂	381296.8	305037.4	381296.8	305037.4	78.4
O ₂	114408.7	80086.1	95780.9	67046.7	17.2
CO ₂	982.1	500.0	31479.3	16025.8	4.1
CO	0.0	0.0	1487.4	1190.0	0.30
H ₂ O _{vap}	803.6	1000.0	17683.4	22006.0 (5.65% of the dry material)	
Total	828201.4		828005.1		

TABLE 3. Heat Balance

Balance item	Input		Output	
	MJ/ton	%	MJ/ton	%
Natural gas	74.51	6.02	0.00	0.00
Solid fuel	688.32	55.61	0.00	0.00
Charge (60°C)/cake	85.02	6.87	78.86	6.31
Air/outgoing gases	68.38	5.52	744.27	59.54
Dissociation of CaCO ₃	0.00	0	125.15	10.01
Evaporation of H ₂ O	0.00	0	176.07	14.08
Oxidation of FeO	321.49	25.97	0.00	0.00
Heating of the grates and pallets	0.0	0	125.78	10.06
Total	1237.72	100	1250.13	100

3) it is possible to calculate and visualize the temperature distribution, the distribution of negative pressure, and the distribution of flue-gas flow rate either in individual vacuum chambers or groups of vacuum chambers;

4) values can be assigned for the distributions of the coarseness and bulk density of the charge, as well as the concentration of solid fuel over the height of the bed;

5) the ratio of CO and CO₂ formed during combustion of the carbon in the fuel can be correlated with the calorific value of the fuel that is being burned inside the bed;

TABLE 4. Partial Material Balances, kg/h

Element	Oxygen balance		Carbon balance		Iron balance		Calcium balance		Hydrogen balance	
	Input	Output	Input	Output	Input	Output	Input	Output	Input	Output
CaCO ₃	8080	26.5	2020.1	6.6			6738	22		
MgCO ₃	0.0	0.0	0.0	0.0						
FeO	8624	7082			30182	24788				
CaO	3948	6633					9871	16582		
MgO	1265	1265								
Fe ₂ O ₃	41604	43916			97076	102470				
Water	15004								1876	0.0
O ₂	114409	95781								
CO ₂	714	22894	268	8585						
CO	0.0	850	0.0	638						
H ₂ O _{vap}	714	15719							89	1965
Coke fines			8467	1526						
Total	194363	194166	10755	10756	127258	127258	16609	16604	1965	1965
Error	1.253	196.79	0.76	0.77	2.27·10 ⁻⁴	0.30	-1.9·10 ⁻⁶	-7.3·10 ⁻²	1.39·10 ⁻²	1.44·10 ⁻²

TABLE 5. Parameters of the Gas Flow ahead of the Blowers

Blower	Negative pressure, kPa	Temperature, °C	Flow rate, nm ³ /h / m ³ /h	Air infiltration, nm ³ /h	Composition of the gas, %				
					N ₂	O ₂	CO ₂	CO	H ₂ O
Sintering zone	12.32	119.2	481853 / 785971	151862 (31.5%)	74.78	17.08	3.32	0.25	4.57
Cooling zone	8.22	165.5	524391 / 915069	197030 (37.6%)	79.08	20.92			

6) heat transfer between the bed and the pallets can be accounted for; and

7) recirculation of the flue gases from the sintering zone and the use of heat from the medium that is used to cool the sinter can both be calculated.

Figure 3 shows the results obtained from adaptation of the model based on the temperature of the flue gases and the vacuum in the vacuum chambers. The results are shown for two characteristic operating regimes of the sintering machine at the ChMK.

Table 1 shows the main operating parameters of the machine in the base regime. Tables 2–4 show the total and partial material balances and the total heat balance for the adapted operating regime of the machine, and Table 5 shows the parameters of the gas flow ahead of the machine's blowers.

The calculated and experimental data agree well with the actual values of the machine's operating parameters and can be used for theoretical studies and the solution of practical problems (see Part II).

REFERENCES

1. H. B. Wendeborn, "Symposium on Sinter," *Spec. Rep. Iron and Steel Inst.*, No. 53, 1–9 (1955).
2. E. W. Voice and R. Wild, *Second Symp. Inter. sur l'agglomeration des mineraux de fer. IRSID*, Paris (1957), pp. 7–30.
3. A. Anzelius, *Z. Angew. Math. Mech.*, **6**, No. 1, 291–298 (1926).
4. T. Schuman, *J. of the Franklin Inst.*, **208**, 425–426 (1929).
5. S. G. Bratchikov, S. V. Bazilevich, Yu. G. Yaroshenko, and G. M. Maizel, *Izv. Vyssh. Uchebn. Zaved. Chern. Metall.*, No. 6, 18–26 (1963).
6. Yu. A. Frolov, "Heat-engineering aspects of the sintering process," *Stal*, No. 12, 2–11 (2003).
7. F. R. Shklyar, V. M. Malkin, B. A. Bokovikov, et al., *Metallurgical Heat Engineering: Sci. Works of VNIIMT, Metallurgiya*, Moscow (1979), No. 8, pp. 119–127.
8. M. J. Cumming and J. A. Thurlby, "Developments in modeling and simulation of iron ore sintering," *Ironmak. Steelmak.*, **17**, No. 4, 245–254 (1990).
9. N. K. Nath, A. J. Silva, and N. Chakraborti, "Dynamic process modeling of iron ore sintering," *Steel Res.*, **68**, No. 7, 285–292 (1977).
10. J. Mitterlehner et al., "Modeling and simulation of heat front propagation in the iron ore sintering process," *ISIJ Int.*, No. 44, 11–20 (2004).
11. H. Yamaoka and T. Kawaguchi, "Development of a 3D sinter process mathematical simulation model," *ISIJ Int.*, No. 45, 522–531 (2005).
12. J. A. Castro, A. J. Silva, H. Nogami, and J. Yagi, "Modelo matematico tridimensional multifasico da geracao de dioxinas no leito de sinterizacao," *TMM – Tecnol. Metal. Mater.*, No. 2, 45–49 (2005).
13. J. A. Castro, Y. Sasaki, and J. Yagi, "Three dimensional mathematical model of the iron ore sintering process based on multiphase theory," *Mater. Res.*, No. 15, 848–858 (2012).
14. Yu. A. Frolov, L. I. Polotskii, V. A. Kobelev, and V. V. Konoplyanik, "Three dimensional dynamic model of the sintering process," *Chern. Metall.: Byull. NTiEI*, No. 11, 29–30 (2005).